THE JOURNAL OF PHYSICAL CHEMISTRY B

Article

pubs.acs.org/JPCB

Solid-State NMR ^{31}P Paramagnetic Relaxation Enhancement Membrane Protein Immersion Depth Measurements

Sergey Maltsev, Stephen M. Hudson, Indra D. Sahu, Lishan Liu, and Gary A. Lorigan*

Department of Chemistry and Biochemistry, Miami University, Oxford, Ohio 45056, United States

ABSTRACT: Paramagnetic relaxation enhancement (PRE) is a widely used approach for measuring long-range distance constraints in biomolecular solution NMR spectroscopy. In this paper, we show that ^{31}P PRE solid-state NMR spectroscopy can be utilized to determine the immersion depth of spin-labeled membrane peptides and proteins. Changes in the ^{31}P NMR PRE times coupled with modeling studies can be used to describe the spin-label position/amino acid within the lipid bilayer and the corresponding helical tilt. This method provides valuable insight on protein−lipid interactions and membrane protein structural topology. Solid-state ^{31}P NMR data on the 23 amino acid α-helical nicotinic acetylcholine receptor nAChR M2δ transmembrane domain model peptide followed predicted behavior of ^{31}P PRE rates of the phospholipid headgroup as the spin-label moves from the membrane surface toward the center of the membrane. Residue 11 showed the smallest changes in ^{31}P PRE (center of the membrane), while residue 22 shows the largest ^{31}P PRE change (near the membrane surface), when compared to the diamagnetic control M2δ sample. This PRE SS-NMR technique can be used as a molecular ruler to measure membrane immersion depth.

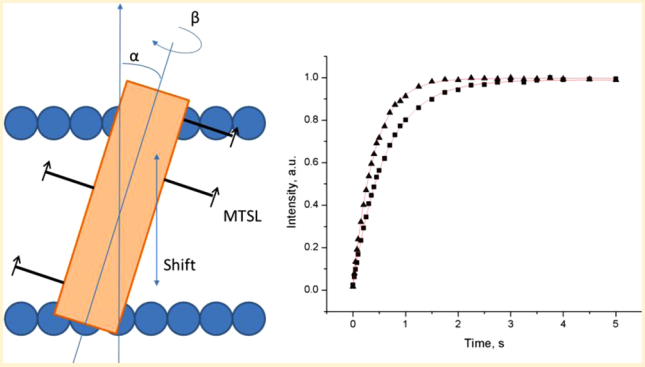

INTRODUCTION

Studying a membrane protein inside or on the surface of a lipid membrane is a challenging task. The complexity of the protein−lipid system, its dynamics and in most cases experiment has to be performed under physiological conditions, limit the use of conventional biophysical methods such as X-ray crystallography. A great number of topologies that a protein can adopt in a lipid environment are known already; e.g., membrane embedded helices can span through the bilayer or form various loops, they can enter at different angles into the membrane, they can be short or kinked or interrupted, etc.[1] Exact protein location and topology within the membrane, its orientation, and solvent exposure of its residues are crucial pieces of information for both membrane embedded and membrane anchored proteins. In the case of antimicrobial peptides, whose activity can result in the rupture of lipid membranes, it is important to characterize how exactly and at which concentrations the peptides proceed from a surface bound to a channel forming state.[2] For membrane proteins, in order to understand their functionality, it is also important to follow their dynamic properties, as they may change both their orientation and position in the membrane.[3]

Such detailed information, however, is challenging to access with conventional methods like fluorescence,[4−7] FTIR,[8] EPR,[9−12] or scanning cysteine accessibility mutagenesis techniques.[13−15] In the case of fluorescence and EPR, the precision is limited to 1.5−3.0 Å due to the size of the fluorescent probe or spin-label, respectively. In the case of EPR distance measurement experiments like ESEEM[16] or DEER,[17] a sample has to be cooled down to liquid nitrogen temperature or lower, which brings it far away from physiological conditions (some recent findings show that it is possible in some cases to collect DEER measurements at room temperature[18]). In the case of scanning cysteine accessibility mutagenesis, the technique provides qualitative results on a protein embedding by discrimination between the intra- and extracellular location of a certain domain of the protein.

With ^{31}P NMR data of phospholipids, however, it is possible to conduct relaxation experiments at any temperature. In addition, ^{31}P nuclei are 100% naturally abundant and have a relatively high gyromagnetic ratio. Thus, ^{31}P NMR spectra can be acquired relatively fast with an outstanding signal-to-noise ratio, making it an excellent target isotope. Introducing strong paramagnetic species into a sample helps to overcome the problem of short distance interactions. A paramagnetic label will interact with surrounding atoms via a dipole−dipole coupling mechanism, which can be probed by a number of well-established NMR techniques like PRE, PCS, etc.[19−22] Distance information can be determined from such coupling measurements with potential limits up to 20 Å.[19] Over the past decade, inclusion of paramagnetic species in biological systems gained increasing popularity in biochemical NMR research in three directions: site-directed spin-labeling (SDSL), where in most cases a nitroxide spin-label is attached to a molecule of interest (applications include but are not limited to protein assignments and fold determination),[23−25] dissolution of paramagnetic

Received: January 9, 2014
Revised: April 1, 2014
Published: April 1, 2014

Figure 1. nAChR M2δ amino acid sequence. Spin-labeled positions are marked with the blue color.

species in order to study the surface properties of molecular assemblies,[26−31] and high-pressure ^{17}O dissolution which is known to enter and concentrate inside a lipid bilayer in a gradient manner.[32,33] Previous NMR studies showed a possibility of protein depth estimation based on lipid ^{13}C PRE from dissolved Mn^{2+},[27] but the dephasing curves were nonlinear and challenging to analyze.

Thus, new experimental biophysical methods are needed that will greatly facilitate the process of obtaining residue-specific information on protein−membrane complexes. Most NMR interactions are rather short ranged, and EPR spectroscopy does not provide enough specificity. The right combination of them, however, combines their strengths and can be utilized to develop a technique that will successfully address both the topology and immersion depth questions.

Here we present an extension of our previously published work on phospholipids[34] to a membrane peptide in a phospholipid bilayer. We show that the lipid headgroup ^{31}P PRE induced by nitroxide spin-labels at different amino acid positions of a protein can serve as a molecular ruler inside the lipid bilayer for protein immersion depth calculations.

For our purposes, we have chosen the δ-subunit of the transmembrane segment M2 of nicotinic acetylcholine receptor (M2δ nAChR), as it is well studied[35−41] and is often used as a model membrane protein system (Figure 1). Opella et al. report a 12° tilt of the protein inside DMPC bilayers that has been measured with PISEMA NMR and oriented bilayers deposited on the glass slides which was in agreement with the structure from the electron diffraction map.[42] No other published result on the tilt angle in different lipid environments is available at the moment. However, the depth of insertion has not been directly tested. In order to measure it, we have synthesized a wild-type sample as well as a set of mutants with Cys-substituted amino acids at positions 3, 5, 6, 9, 11, 12, 16, 18, 20, 21, and 22. The Cys mutants were spin-labeled with MTSL and reconstituted into POPC multilamellar vesicles (MLVs). Measured ^{31}P PRE NMR rates showed a smooth and predictable behavior over the whole range of immersion depths, making it easy to map the relaxation enhancements to immersion depths. Another set of samples was prepared to verify how sensitive the relaxation data are to exact the sample preparation conditions.

MATERIALS AND METHODS

nAChR M2δ peptide samples were synthesized with a CEM Liberty Microwave-Enhanced Peptide Synthesizer using Fmoc-protection chemistry.[34,43,44] Each sample, except for the wild type, had one of its amino acids replaced with a cysteine. Nine different positions along the amino acid sequence were selected for Cys mutations: 3, 6, 9, 11, 14, 16, 18, 20, and 22. The peptides were cleaved from the resin by a 20 mL cleavage solution containing 85% TFA (trifluoroacetic acid), 5% water, 5% anisole, and 5% triisopropylensilane. A CEM Discovery Microwave unit and CEM Accent accelerated the cleavage process by running for 30 min at 38 °C with a stir bar at high speeds.

The peptide−resin mixture was filtered. Excess TFA was gently evaporated off by passing pure N_2 gas over it for 2−3 h. To remove the rest of the solvents, ice-cold methyl *tert*-butyl ether was added, ice bathed for 30 min, centrifuged for 10 min, and the supernatant poured off. The ether wash was repeated three times in total, and then, the resulting precipitate was lyophilized overnight.

The crude protein was purified with a GE AKTA HPLC system using a reverse-phase preparation size C4 column (Vydac cat. # 214TP1022). The solvent system consisted of H_2O with 0.1% TFA (solvent A) and a mixture of 90% acetonitrile and 10% water with 0.1% TFA (solvent B). Fractions collected from the corresponding HPLC peaks were lyophilized to yield pure protein. MALDI-TOF data were collected to confirm that the sample had the correct molecular weight.

In order to label with MTSL, the protein was dissolved in DMSO (dimethyl sulfoxide). MTSL (*S*-(2,2,5,5-tetramethyl-2,5-dihydro-1*H*-pyrrol-3-yl)methylmethanesulfonothioate spin-label) purchased from Toronto Research Chemicals was added with 10 molar excess to the peptide solution. The sample was sonicated, then stirred for 24 h at room temperature, and lyophilized until full removal of DMSO. HPLC was run to purify the labeled protein, and MALDI-TOF data was used to confirm the resultant molecular weight of the peptide.

Each multilamellar vesicle sample was prepared with 5 wt % protein/lipids and vacuum-dried overnight. POPC (1-palmitoyl-2-oleoylphosphatidylcholine) lipids were purchased from Avanti Polar Lipids Inc. A buffer solution was prepared with 1.17 mg of NaCl, 7.15 mg of HEPES, and 1 mL of deuterium depleted H_2O, resulting in a 20 mM solution of salt and a 30 mM buffer. The pH was then adjusted to 7 with NaOH. The buffer was added to the sample in a ratio of 20 μL for each 1 mg of protein. Five freeze/thaw cycles were performed consisting of 1 min of freezing in liquid nitrogen, 3 min of thawing at 50 °C, and 2 min of vortexing.

The quality of MLVs was assessed by dynamic light scattering (DLS) and static ^{31}P direct acquisition single pulse experiments, producing the well-known powder pattern without any sign of isotropic component.[45] Typical vesicle sizes by DLS results were around 400 nm in diameter.

Four reference samples with wild-type protein and DOXYL-labeled lipids were made with 5 mol % protein/lipid and 5 mol % spin-labeled lipid/lipid. The lipids in these samples were Avanti DOXYL PC lipids, each labeled at a different carbon number: 5, 7, 10, or 12. The same sample protocol was used as described for the MTSL labeled protein samples. Two wild-type samples and three unlabeled cysteine-mutated samples at position 18 were made to demonstrate the reproducibility of relaxation results.

All samples were centrifuged into standard 4 mm Bruker rotors. All NMR data were collected on a Bruker AVANCE 500 MHz wide-bore NMR spectrometer equipped with a BRUKER triple CP-MAS probe. ^{31}P longitudinal relaxation times (T_1) were measured at 5 kHz MAS speed using a standard quasi-2D direct ^{31}P saturation recovery pulse sequence with 64 saturation loops, 10 ms saturation delay, and 7 μs 90° pulses. 32 T_1 points

dx.doi.org/10.1021/jp500267y | J. Phys. Chem. B 2014, 118, 4370−4377

in indirect dimension were collected for each sample with variable delay ranging from 1 ms to 5 s. The data were fitted with one exponent model in standard Bruker Topspin software. Several samples were made in duplicate, while a total of six samples were prepared and measured for the wild-type case to establish the uncertainty in the relaxation measurements. PRE relaxation curves were measured with saturation recovery pulse sequence, and the resulting curves were fitted in Igor Pro with a single exponential model.

Theoretical Description. A very good description of the relaxation processes occurring within the lipid membranes is given in the literature.[46] Klauda et al. have shown that for strong magnetic fields (>2 T) longitudinal relaxation rates for ^{31}P of lipids are dominated by CSA relaxation, rather than by dipolar coupling with the proton bath. However, the situation changes when we incorporate a large magnetic dipole such as a spin-label. The strong dipolar coupling (657 times stronger than protons) in this case adds another relaxation mechanism to the system that depends on the distance between phosphorus atoms and the spin-label.

PRE in NMR is well studied[19−21,23,31,34] and is a widely used phenomenon. Most applications, however, are more qualitative rather than quantitative, e.g., obtaining structural constraints and topology information from ^{1}H or ^{13}C PRE in NMR of proteins,[47] resonance assignments,[48,49] protein−protein and protein−ligand interactions,[50−52] conformational heterogeneity and exchange,[53] etc. Other paramagnetically induced phenomena like pseudocontact shifts (PCS) and residual dipolar couplings (RDC) work better in the liquid state NMR than in the solid state due to moderate line broadening and restricted mobility in the latter case. Spin−lattice relaxation enhancement, however, does not depend on the spectral line width or mobility of the system, making it an excellent candidate for quantitative studies.

The general theory of paramagnetic relaxation enhancement in materials with paramagnetic impurities was founded by Blumberg[54] and Goldman[55] in 1959−1965 following works of Bloembergen[56] and van Vleck.[57] They calculated the transition probability of a nucleus at a certain distance from the paramagnetic center (averaged over the angular dependence):

$$P(r) = \frac{1}{5\pi}(\gamma_P\gamma_n\hbar)^2 S(S+1) r^{-6} \frac{\tau}{1+\omega^2\tau^2} = Cr^{-6} \quad (1)$$

where γ_P and γ_n are gyromagnetic ratios of the paramagnetic center and the corresponding nucleus, r is the distance between the two, S is the spin of the paramagnetic center, τ is the electron correlation time of the paramagnetic center, and ω is the nuclear Larmor frequency.

The total relaxation rate of the nuclei can be defined as

$$R = R_{ref} + R_{PRE} \quad (2)$$

where R_{ref} is the relaxation rate of a diamagnetic (no spin-label) control sample and R_{PRE} is the actual paramagnetically induced relaxation enhancement. R_{PRE} can be separated into two components: the actual PRE of an atom at a certain distance from the paramagnetic center (R_{PRE}^{a}) and the relaxation enhancement rate due to spin duffusion (R_{SD}). R_{PRE}^{a} can be described in terms of the transition probability of a nucleus at a certain distance from the paramagnetic center given in eq 1 and will be used for calculations of the spin-label depths inside the membrane, while R_{SD} can be calculated for a set of samples prepared in the same way and measured under the same conditions so their spin-label concentration, lipid vesicle architecture, and mobility are the same.

Blumberg in his works has distinguished three modes of impurity controlled relaxations based on spin-diffusion speed: (i) no spin diffusion, (ii) limited spin diffusion, and (iii) rapid spin diffusion. This theory was developed for rigid crystalline samples, and in the case of phospholipid vesicles was found to be quite rapid (compared to typical ^{31}P spin−lattice relaxation time), where lipid lateral diffusion up to 8.6×10^{-8} cm^2/s occurs.[58] Without any kind of diffusion, the ^{31}P NMR spin−lattice relaxation of a lipid sample (independently of protein presence) should yield a curve representing several components, resulting from lipid head groups placed at different distances from the paramagnetic center governed by eq 1. Such curves would be very hard to analyze due to a complex multiexponent behavior. MLVs at room temperature, however, do show very nice single-exponential behavior (Figure 2) that

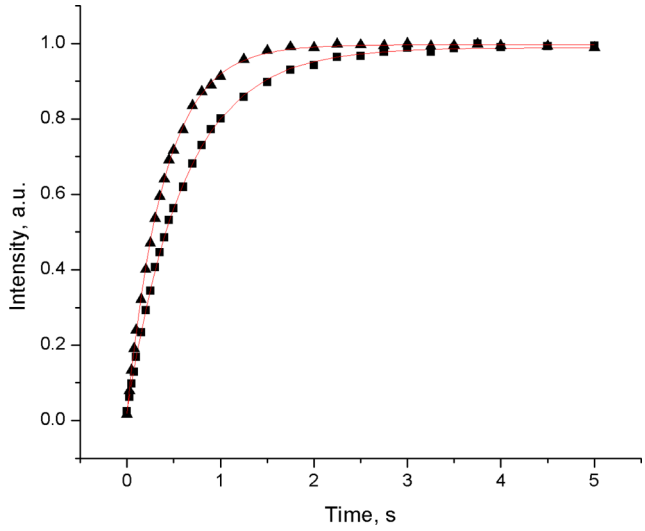

Figure 2. An example of ^{31}P T_1 PRE fit. 32 time increments were used for all samples. The fit for the M2δ11 sample is shown with τ = 0.603 ± 0.006 s as squares and the M2δ22 sample with τ = 0.384 ± 0.008 s as triangles with corresponding single-exponential fits.

clearly shows the effect of the diffusion processes. Such an averaging can also be exploited in order to estimate the strength of lipid−protein interactions; e.g., in the case of strong interactions when nearby lipids cannot diffuse at the common rate, a second, fast-relaxing component can appear in the T_1 graph. In our case, the NMR experiments indicate that the lipid lateral diffusion speed is enough to produce just one relaxation component.

When no spin-label is present in the sample, the ^{31}P spin diffusion also helps to average the relaxation rate. However, in spin-labeled samples, it also helps to increase the overall relaxation rate by "draining" the polarization toward the ^{31}P atom that is closest to the paramagnetic center. The value of the nuclear spin diffusivity was estimated by Bloembergen:[56]

$$D \cong \frac{a^2}{50T_2} \quad (3)$$

where a is the typical ^{31}P−^{31}P internuclear distance, which is estimated to be $(67)^{1/2}$ Å for POPC lipids at room temperature,[59] and T_2 is the transverse relaxation time of the nuclei. The T_2 value can be measured with Hahn echo or

dx.doi.org/10.1021/jp500267y | J. Phys. Chem. B 2014, 118, 4370−4377

CPMG experiments. In order to calculate the corresponding relaxation rate correction factor, first we have to calculate the "exclusion radius"[55] defined by Khutsishvili[60] as

$$b = 0.68\left(\frac{C}{D}\right)^{1/4} \tag{4}$$

where C is the constant in eq 1 and D is the nuclear spin diffusivity from eq 3. Thus, the relaxation rate correction is

$$R_{SD} = 4\pi NbD \tag{5}$$

where N is the spin-label concentration. For a typical value of T_2 = 200 μs and 5 mol % spin-label concentration in POPC lipids, R_{SD} is 0.2 Hz.

The equation for the nuclear spin magnetization density is given by

$$\frac{\partial\rho}{\partial t} = D\nabla^2\rho - C(\rho - \rho_0)\sum_n (\mathbf{r} - \mathbf{r}_n)^{-6} \tag{6}$$

where $\mathbf{r}_n$ is the location of the nth phosphorus atom around the paramagnetic center positioned at $\mathbf{r}$ and ρ_0 is the equilibrium value of ρ. In general, the total nuclear magnetization after time t is obtained by integration of the solution of eq 6 by sample volume. On short intermolecular distances, however, we have to take into account real ^{31}P spin-label distance distributions, rather than averaged by the sample volume phosphorus atom density which will give a singularity at the spin-label position. From geometric considerations based on lipid headgroup size and spin-label depth, it can be estimated how much the PRE effect will be for the nearest, second nearest, and other phosphorus atoms. Such calculations for the cases of the protein labeled at positions 3 and 11 are presented in Figure 3. It is clearly seen that the error of the PRE calculation drops fast as more atoms are included in the calculation and it is generally safe to consider the first five nearest atoms even for the case of a spin-label very close to the surface for the theoretical calculation of the PRE curve with 2% accuracy. In the case of experimentally measured values, the result indicates that R_{PRE}[a] contains mostly information about only several closest phosphorus atoms and can be utilized to study protein−lipid interactions. From this, it is easy to deduce the immersion depth of the spin-label inside the lipid bilayer:

$$d = \left(\frac{C}{R_{exp} - R_{ref} - R_{SD}}\frac{\tau}{1 + \omega^2\tau^2}\right)^{1/6} \tag{7}$$

To calculate the corresponding backbone position from the PRE data, it is also necessary to know the size of the spin-label and the protein tilt angle. Protein tilt, however, as well as protein shift inside the bilayer can be calculated from a set of PRE measurements with different spin-labeled positions.

In order to get relaxation rates from molecular dynamics simulations, a PRE effect was calculated for every ^{31}P atom of every simulation frame and then averaged for the number of frames. Due to the rapid lateral diffusion of the lipid molecules when compared to the NMR experimental time, a simplifying assumption was made that during the course of the experiment every lipid molecule can be found at any other lipid molecule's position in the simulation. First, such a simplification allows the simulation time to be significantly decreased, and second, it is reasonable because at diffusion rates of around 10 $\mu m^2/s$[58] the simulation time of 10 ns is enough to sample the local movements of most lipid molecules. It has to be taken into account, however, that 10 ns is not enough to sample all of the molecular motions and motional states, and therefore simulation results have to be considered with care.

The total relaxation rate following eq 1 can be calculated as

$$R_{sim} = R_{ref} + R_{SD} + \mathrm{Conc}\frac{1}{N_{Frames}}\sum_{N_P}\sum_{N_{Frames}} P(r_n) \tag{8}$$

where Conc is the spin-label concentration relative to the amount of lipid molecules, N_{Frames} is the number of frames in the simulation, N_P is the number of all ^{31}P atoms present in the simulation, and r_n is the distance between the nth phosphorus atom and the spin-label.

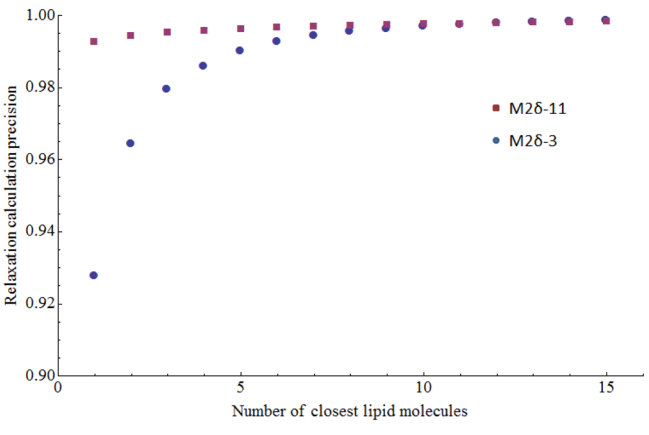

Figure 3. Theoretical PRE effect calculated for different numbers of lipid molecules closest to the spin-labeled protein molecule. 100% is calculated for the case when all lipid molecules are considered for PRE calculation. When the spin-label is located close to the bilayer surface (M2δ-3 case), the same number of neighboring lipids produces a bigger error than for the case of a centrally located spin-label (M2δ-11). On the basis of reproducibility of experimental results, 2−3% error in PRE calculation in general can be achieved with less than five lipid molecules taken for the calculation.

RESULTS AND DISCUSSION

^{31}P is an excellent NMR probe of biomolecules due to its relatively high gyromagnetic ratio, 100% natural abundance, location in the lipid headgroup region, and relatively fast T_1 relaxation in lipids, usually on the order of seconds. ^{31}P PRE NMR membrane depth measurements were conducted on 24 M2δ protein samples incorporated into POPC MLVs. Samples were spin-labeled at the following positions: 3, 5, 6, 9, 11, 12, 16, 18, 20, 21, and 22. A control wild-type sample was prepared without a spin-label. The relaxation data for positions 11 and 22 are displayed in Figure 2. The M2δ sample spin-labeled at position 22 has a shorter T_1 value (384 ms, see Table 1) when compared to position 11 (603 ms), because it is located closer to the membrane surface. The M2δ sample spin-labeled at position 11 is buried near the center of the membrane and still has a T_1 value smaller than the WT control sample (694 ms).

The ^{31}P NMR relaxation data collected in this study were well fit with a single exponential to glean out the corresponding T_1 values. This is surprising given the number of ^{31}P nuclei in a phospholipid bilayer poised at different positions and distances relative to the spin-labeled protein. The overall position of a spin-label relative to the ^{31}P atoms and overall dynamics of the system need to be considered. Figure 3 shows the theoretical/computational ^{31}P PRE effect calculated as a function of the

dx.doi.org/10.1021/jp500267y | J. Phys. Chem. B 2014, 118, 4370−4377

Table 1. ^{31}P Experimental PRE Data Fitting Results

spin-label position	relaxation time (s)
3	0.490 ± 0.008
5	0.459 ± 0.006
6	0.531 ± 0.007
9	0.566 ± 0.008
11	0.603 ± 0.006
12	0.570 ± 0.007
16	0.528 ± 0.008
18	0.531 ± 0.006
20	0.473 ± 0.008
21	0.503 ± 0.008
22	0.384 ± 0.008
wild type (average of five samples)	0.694 ± 0.002

number of ^{31}P lipid molecules with spin-labeled M2δ at positions 3 and 11. A total of 32 data points per relaxation curve were calculated in order to eliminate possible issues with the number of relaxation components. Taking lipid lateral diffusion into account, which is on the order of 10^{-6}–10^{-7} cm^2/s,[46,58] it becomes clear that, unless a lipid molecule is strongly attached to a protein so it does not diffuse, their natural diffusion within the bilayer will effectively average out all the relaxation differences during the course of the NMR measurement, which takes on the order of a fraction of a second to several seconds. This explains why the data were easily fit with a single exponential.

Resulting ^{31}P NMR PRE values for several mutated positions of the M2δ protein are presented in Figure 4A in a bar graph format. The green bars show the ^{31}P T_1 PRE % when compared to a control sample, while the blue bars represent the best structural modeling results with a 12° helical tilt of M2δ with respect to the membrane. For comparison, Figure 4B shows the same modeling procedure used for the M2δ protein with a 0° helical tilt with respect to the lipid bilayer (perpendicular to the bilayer surface). Figure 4B is a good example of what relaxation behavior can be expected at different immersion depths. It is clearly seen in this case that the relaxation enhancement is a smooth function of the spin-label depth inside the bilayer and has enough sensitivity to pinpoint spin-label positions clearly discriminating different labeling sites or residues. Due to the natural nonlinearity of the PRE effect, the most sensitivity is achieved for the labeled positions close to the membrane surface, whereas the difference between most immersed spin-labels is somewhat diminished.

In order to probe the structural properties of the protein within the lipid bilayer and their effect on PRE, we developed a straightforward model that describes the whole complex. An α-helix of the protein was taken as a rigid cylinder of corresponding size (the Cα–Cα diameter was set at 5.4 and 34 Å length), and all MTSL labels were placed perpendicular to the cylinder axis with 8 Å length (equal to the distance between Cα and N of MTSL) (Figure 5). This model worked well for predicting the corresponding ^{31}P PRE lipid relaxation times.[46] A pentamer of protein models was placed in a lipid bilayer, and the PRE effect was calculated for all labeled positions. Parameters to fit were the tilt angle α, roll angle β, vertical shift S inside the membrane, and electron correlation time τ_c. The phospolipids were modeled as a sparse network of 15 ^{31}P atoms around the protein on both sides of the bilayer. The number 15 was chosen on the basis of the error estimation coming from the fact that at the same time several ^{31}P atoms

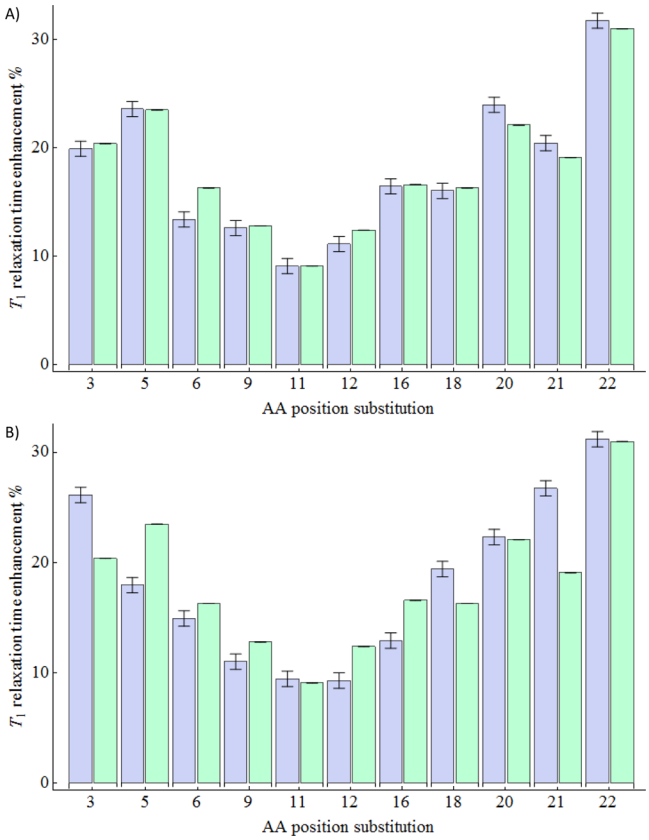

Figure 4. Relaxation enhancement of the M2δ–MTSL complex. Experimental results (green) and model fitting (blue): (A) case of 12° protein tilt inside the bilayer; (B) modeled 0° protein tilt (experimental green bars are the same as in part A).

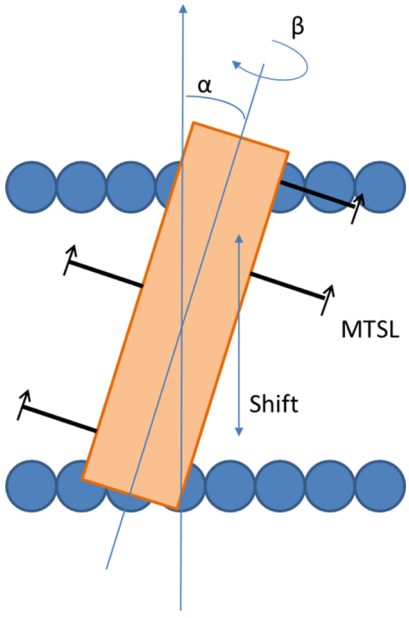

Figure 5. Protein in the lipid bilayer model. All experimentally available spin-labels were put on the model protein to be fitted simultaneously. For details, see the text.

will be affected by the spin-label and therefore will have different momentary relaxation rates. Figure 3 shows how the error in PRE calculations depends on the number of lipid molecules considered and the spin-label position. In order to

dx.doi.org/10.1021/jp500267y | J. Phys. Chem. B 2014, 118, 4370–4377

account for the diffusion processes, a simple assumption was made that all lipids are equally mobile during the course of the NMR experiment (i.e., have the same lateral diffusion speed and the incorporation of the peptide does not affect it). This assumption basically means that all lipid molecules will find themselves in all of the accounted 15 lipid positions equally, which allows us to easily calculate a single relaxation rate. Such an assumption should be valid for the majority of the protein/lipid systems.[61]

Experimental results from all spin-labeled positions to the ^{31}P atoms were fit globally. The results of the fitting are presented in Figure 4A. As seen from the graph, this simple model fits very well with the experimental results and agrees well with the results from the literature: a tilt angle of 12° is known for nAChR M2δ,[42] and the N-terminus side of the peptide is shifted closer to the membrane headgroup (1.5 Å shift estimated) due to a higher concentration of polar amino acids at that end and was theoretically predicted by Amit Kessel et al.[62]

No deviation from the straight helix was observed on the basis of fitting results, which corresponds to the majority of the results for nAChR M2δ in POPC vesicles from the literature.[35,42,63,64] The M2δ helix is known to rotate rapidly along its helical axis[65] when in monomeric form. It is known that under physiological peptide concentrations it tends to form pentamers and this type of rotation is hindered due to the interaction of neighboring helices which results in "kinky" rather than smooth behavior of the relaxation curve in Figure 4A, when compared to Figure 4B. This can be seen as indirect evidence for pentamerization of the peptide at higher concentrations.

An area of uncertainty in these membrane depth measurements lies in an estimation of the electron correlation time τ_c. Several methodologies have been used to determine τ_c. First, it is temperature dependent and can be obtained from several T_1 measurements at different temperatures. In this case, however, it is also necessary to consider the temperature dependence of R_{ref} and R_{SD} as well as lipid mobility changes and phase transitions. Also, it can be obtained with a combination of both T_1 and T_2 measurements,[19] but lipid samples usually have very short T_2 values that are not easy to measure precisely and in the static case it tends to be anisotropic consisting of several different components. MAS measurements of T_2 are also not a good option because short T_2 values have to be measured at very high spinning speeds to get reasonable resolution and several points on the corresponding relaxation curve. Third, τ_c can be deduced from measurements of the same sample at different magnetic fields. All of these methods, however, can be used to give approximate values of the correlation time for our model fitting. Our method proposes another way to calculate τ_c based on fitting R_{SD} and R_{PRE}^{a} simultaneously. Indeed, both of them depend on τ_c, but while R_{SD} governs the size of the gap, R_{PRE}^{a} governs the incline of the "wings". Such simultaneous fitting gives high precision and is straightforward. The calculated value for τ_c of 12 ns was found to be well in the range for nitroxide spin-labels.[66] It is, however, for the first time that τ_c was calculated for a real biologically relevant sample using this technique.

CONCLUSIONS

We have presented a novel method for membrane protein topology and immersion depth based on site-directed spin-labeling and paramagnetic relaxation enhancement ^{31}P NMR. The method can be utilized as a *molecular ruler* to measure positions of labeled amino acids within the lipid membrane. It allows precise determination of the spin-label immersion depth, and hence, membrane protein structural and topological properties can be measured under physiological conditions. The method shows predictable behavior of the relaxation rate enhancements depending on the paramagnetic center immersion depth, making it easy to interpret the data. It also allows for an easy and precise calculation of the electronic correlation time, which is otherwise an elusive quantity that can be useful in other experiments: some PRE based spectroscopic distance measurement methods rely on precise knowledge of the electronic correlation time. The NMR data are presented for a set of samples with nAChR M2δ protein mutated at different positions, showing the applicability of the method to complex biological systems. Particularly, it was shown that the peptide tends to take a shifted position within the bilayer with the N-terminus shifted 1.5 Å closer to the lipid surface than the other C-terminus. A theoretical background is given describing the phenomena and their relevance behind the PRE in lipid vesicles as well as error estimation from different sources for calculation. This method can be further explored by replacing PCs by PEs. The stronger lateral interaction between the PEs may reflect how the interfacial process is involved. Another possibility is to test lipid in the gel phase in which the water amount and lateral interactions of the head groups are considerably altered with respect to the liquid crystal.

AUTHOR INFORMATION

Corresponding Author

*E-mail: gary.lorigan@MiamiOH.edu. Phone: 1-513-5293338.

Notes

The authors declare no competing financial interest.

ACKNOWLEDGMENTS

This research project was supported by NIGMS/NIH (GM108026), R01 GM080542, NSF (CHE-1011909), and MRI-0722403.

REFERENCES

(1) von Heijne, G. Membrane-protein Topology. *Nat. Rev. Mol. Cell Biol.* **2006**, *7*, 909−918.

(2) Brogden, K. A. Antimicrobial Peptides: Pore Formers or Metabolic Inhibitors in Bacteria? *Nat. Rev. Microbiol.* **2005**, *3*, 238−250.

(3) Prosser, R. S.; Evanics, F.; Kitevski, J. L.; Patel, S. The Measurement of Immersion Depth and Topology of Membrane Proteins by Solution State NMR. *Biochim. Biophys. Acta* **2007**, *1768*, 3044−3051.

(4) Chattopadhyay, A.; London, E. Parallax Method for Direct Measurement of Membrane Penetration Depth Utilizing Fluorescence Quenching by Spin-Labeled Phospholipids. *Biochemistry* **1987**, *26*, 39−45.

(5) Clague, M. J.; Knutson, J. R.; Blumenthal, R.; Herrmann, A. Interaction of Influenza Hemagglutinin Amino-Terminal Peptide with Phospholipid Vesicles: A Fluorescence Study. *Biochemistry* **1991**, *30*, 5491−5497.

(6) Strashnikova, N. V.; Medvedeva, N.; Likhtenshtein, G. I. Depth of Immersion of Fluorescent Chromophores in Biomembranes Studied by Quenching with Nitroxide Radical. *J. Biochem. Biophys. Methods* **2001**, *48*, 43−60.

(7) Posokhov, Y. O.; Ladokhin, A. S. Lifetime Fluorescence Method for Determining Membrane Topology of Proteins. *Anal. Biochem.* **2006**, *348*, 87−93.

(8) Huang, W. N.; Sue, S. C.; Wang, D. S.; Wu, P. L.; Wu, W. G. Peripheral Binding Mode and Penetration Depth of Cobra Cardiotoxin on Phospholipid Membranes as Studied by a Combined FTIR and Computer Simulation Approach. *Biochemistry* **2003**, *42*, 7457−7466.
(9) Dalton, L. A.; McIntyre, J. O.; Fleischer, S. Distance Estimate of the Active Center of D-Beta-Hydroxybutyrate Dehydrogenase from the Membrane Surface. *Biochemistry* **1987**, *26*, 2117−2130.
(10) Monaco, V.; Formaggio, F.; Crisma, M.; Toniolo, C.; Hanson, P.; Millhauser, G. L. Orientation and Immersion Depth of a Helical Lipopeptaibol in Membranes using TOAC as an ESR Probe. *Biopolymers* **1999**, *50*, 239−253.
(11) Nielsen, R. D.; Che, K. P.; Gelb, M. H.; Robinson, B. H. A Ruler for Determining the Position of Proteins in Membranes. *J. Am. Chem. Soc.* **2005**, *127*, 6430−6442.
(12) Carmieli, R.; Papo, N.; Zimmermann, H.; Potapov, A.; Shai, Y.; Goldfarb, D. Utilizing ESEEM Spectroscopy to Locate the Position of Specific Regions of Membrane-Active Peptides within Model Membranes. *Biophys. J.* **2006**, *90*, 492−505.
(13) Bogdanov, M.; Zhang, W.; Xie, J.; Dowhan, W. Transmembrane Protein Topology Mapping by the Substituted Cysteine Accessibility Method (SCAM(TM)): Application to Lipid-Specific Membrane Protein Topogenesis. *Methods* **2005**, *36*, 148−171.
(14) Visudtiphole, V.; Chalton, D. A.; Hong, Q.; Lakey, J. H. Determining OMP Topology by Computation, Surface Plasmon Resonance and Cysteine Labelling: The Test Case of OMPG. *Biochem. Biophys. Res. Commun.* **2006**, *351*, 113−117.
(15) Zhu, Q.; Casey, J. R. Topology of Transmembrane Proteins by Scanning Cysteine Accessibility Mutagenesis Methodology. *Methods* **2007**, *41*, 439−450.
(16) Rowan, L. G.; Hahn, E. L.; Mims, W. B. Electron-Spin-Echo Envelope Modulation. *Phys. Rev.* **1965**, *137*, A61.
(17) Hyde, J. S.; Chen, J. C. W.; Freed, J. H. Electron-Electron Double Resonance of Free Radicals in Solution. *J. Chem. Phys.* **1968**, *48*, 4211.
(18) Zhongyu Yang, Y. L.; Borbat, P.; Zweier, J.; Freed, J. H.; Hubbell, W. Room Temperature Electron Spin Resonance Distance Measurements in T4 Lysozyme Using Trityl-Based Spin Labels. *Biophys. J.* **2011**, *102*, 405a.
(19) Clore, G. M.; Iwahara, J. Theory, Practice, and Applications of Paramagnetic Relaxation Enhancement for the Characterization of Transient Low-Population States of Biological Macromolecules and Their Complexes. *Chem. Rev.* **2009**, *109*, 4108−4139.
(20) Iwahara, J.; Schwieters, C. D.; Clore, G. M. Ensemble Approach for NMR Structure Refinement against H-1 Paramagnetic Relaxation Enhancement Data Arising from a Flexible Paramagnetic Group Attached to a Macromolecule. *J. Am. Chem. Soc.* **2004**, *126*, 5879−5896.
(21) Respondek, M.; Madl, T.; Gobl, C.; Golser, R.; Zangger, K. Mapping the Orientation of Helices in Micelle-Bound Peptides by Paramagnetic Relaxation Waves. *J. Am. Chem. Soc.* **2007**, *129*, 5228−5234.
(22) Su, X. C.; Otting, G. Paramagnetic Labelling of Proteins and Oligonucleotides for NMR. *J. Biomol. NMR* **2010**, *46*, 101−112.
(23) Liang, B. Y.; Bushweller, J. H.; Tamm, L. K. Site-Directed Parallel Spin-Labeling and Paramagnetic Relaxation Enhancement in Structure Determination of Membrane Proteins by Solution NMR Spectroscopy. *J. Am. Chem. Soc.* **2006**, *128*, 4389−4397.
(24) Ellena, J. F.; Moulthrop, J.; Wu, J.; Rauch, M.; Jaysinghne, S.; Castle, J. D.; Cafiso, D. S. Membrane Position of a Basic Aromatic Peptide that Sequesters Phosphatidylinositol 4,5 Bisphosphate Determined by Site-Directed Spin Labeling and High-Resolution NMR. *Biophys. J.* **2004**, *87*, 3221−3233.
(25) Kleerkoper, Q.; Howarth, J. W.; Guo, X. D.; Solaro, R. J.; Rosevear, P. R. Cardiac Troponin-I Induced Conformational-Changes in Cardiac Troponin-C as Monitored by NMR Using Site-Directed Spin and Isotope Labeling. *Biochemistry* **1995**, *34*, 13343−13352.
(26) Shenkarev, Z. O.; Nadezhdin, K. D.; Lyukmanova, E. N.; Sobol, V. A.; Skjeldal, L.; Arseniev, A. S. Divalent Cation Coordination and Mode of Membrane Interaction in Cyclotides: NMR Spatial Structure of Ternary Complex Kalata B7/Mn2+/DPC Micelle. *J. Inorg. Biochem.* **2008**, *102*, 1246−1256.
(27) Buffy, J. J.; Hong, T.; Yamaguchi, S.; Waring, A. J.; Lehrer, R. I.; Hong, M. Solid-State NMR Investigation of The Depth of Insertion of Protegrin-1 in Lipid Bilayers Using Paramagnetic Mn2+. *Biophys. J.* **2003**, *85*, 2363−2373.
(28) Zuleeg, T.; Hartmann, R. K.; Kreutzer, R.; Limmer, S. NMR Spectroscopic Evidence for Mn2+(Mg2+) Binding to a Precursor-Trna Microhelix near the Potential RNase P Cleavage Site. *J. Mol. Biol.* **2001**, *305*, 181−189.
(29) Vander Elst, L.; Muller, R. N. A P-31 and H-1 NMR Relaxometric Study of the Interaction Between Adenosine Triphosphate (ATP) and Paramagnetic Ions (Gd3+ And Mn2+). *Inorg. Chim. Acta* **1998**, *273*, 92−100.
(30) Valensin, G.; Maccotta, A.; Gaggelli, E.; Grzonka, Z.; Kasprzykowski, F.; Kozlowski, H. H-1-NMR and C-13-NMR Investigation of Complexes of Mn2+ with Ocytocin Analogues in (H-2(6))Dimethylsulfoxide. *Eur. J. Biochem.* **1996**, *240*, 118−124.
(31) Roose, P.; VanCraen, J.; Andriessens, G.; Eisendrath, H. NMR Study of Spin-Lattice Relaxation of Water Protons by Mn2+ Adsorbed onto Colloidal Silica. *J. Magn. Reson., Ser. A* **1996**, *120*, 206−213.
(32) Luchette, P. A.; Prosser, R. S.; Sanders, C. R. Oxygen as a Paramagnetic Probe of Membrane Protein Structure by Cysteine Mutagenesis and F-19 NMR Spectroscopy. *J. Am. Chem. Soc.* **2002**, *124*, 1778−1781.
(33) Luchette, P. A.; Prosser, R. S.; Sanders, C. R.; Hancock, R. E. W.; Rozek, A. Membrane Protein Structure By NMR Using Paramagnetic Effects of Oxygen. *Biophys. J.* **2002**, *82*, 516a−516a.
(34) Chu, S.; Maltsev, S.; Emwas, A. H.; Lorigan, G. A. Solid-State NMR Paramagnetic Relaxation Enhancement Immersion Depth Studies in Phospholipid Bilayers. *J. Magn. Reson.* **2010**, *207*, 89−94.
(35) Saiz, L.; Klein, M. L. The Transmembrane Domain of the Acetylcholine Receptor: Insights from Simulations on Synthetic Peptide Models. *Biophys. J.* **2005**, *88*, 959−970.
(36) Huang, L. Transmembrane Nature of Acetylcholine-Receptor as Evidenced by Protease Sensitivity. *FEBS Lett.* **1979**, *102*, 9−12.
(37) Sargent, P. B.; Hedges, B. E.; Tsavaler, L.; Clemmons, L.; Tzartos, S.; Lindstrom, J. M. Structure and Transmembrane Nature of the Acetylcholine-Receptor in Amphibian Skeletal-Muscle as Revealed by Cross-Reacting Monoclonal-Antibodies. *J. Cell Biol.* **1984**, *98*, 609−618.
(38) Giraudat, J.; Montecucco, C.; Bisson, R.; Changeux, J. P. Transmembrane Topology of Acetylcholine-Receptor Subunits Probed with Photoreactive Phospholipids. *Biochemistry* **1985**, *24*, 3121−3127.
(39) Bodereau-Dubois, B.; List, O.; Calas-List, D.; Marques, O.; Communal, P. Y.; Thany, S. H.; Lapied, B. Transmembrane Potential Polarization, Calcium Influx, and Receptor Conformational State Modulate the Sensitivity of the Imidacloprid-Insensitive Neuronal Insect Nicotinic Acetylcholine Receptor to Neonicotinoid Insecticides. *J. Pharmacol. Exp. Ther.* **2012**, *341*, 326−339.
(40) Song, C.; Corry, B. Computational Study of the Transmembrane Domain of the Acetylcholine Receptor. *Eur. Biophys. J. Biophys.* **2009**, *38*, 961−970.
(41) Ortells, M. O.; Barrantes, G. E.; Barrantes, F. J. Molecular Modeling of the Nicotinic Acetylcholine Receptor Transmembrane Region in the Open State. *Biophys. J.* **1996**, *70*, Mp259−Mp259.
(42) Opella, S. J.; Marassi, F. M.; Gesell, J. J.; Valente, A. P.; Kim, Y.; Oblatt-Montal, M.; Montal, M. Structures of the M2 Channel-Lining Segments from Nicotinic Acetylcholine and NMDA Receptors by NMR Spectroscopy. *Nat. Struct. Biol.* **1999**, *6*, 374−379.
(43) Abu-Baker, S.; Lorigan, G. A. Phospholamban and its Phosphorylated Form Interact Differently with Lipid Bilayers: A 31P, 2H, and 13C Solid-State NMR Spectroscopic Study. *Biochemistry* **2006**, *45*, 13312−13322.
(44) Abu-Baker, S.; Lu, J. X.; Chu, S.; Shetty, K. K.; Gor'kov, P. L.; Lorigan, G. A. The Structural Topology of Wild-Type Phospholamban

in Oriented Lipid Bilayers using 15N Solid-State NMR Spectroscopy. *Protein Sci.* **2007**, *16*, 2345−1249.
(45) Abu-Baker, S.; Qi, X. Y.; Lorigan, G. A. Investigating the Interaction of Saposin C with POPS and POPC Phospholipids: A Solid-State NMR Spectroscopic Study. *Biophys. J.* **2007**, *93*, 3480−3490.
(46) Klauda, J. B.; Roberts, M. F.; Redfield, A. G.; Brooks, B. R.; Pastor, R. W. Rotation of Lipids in Membranes: Molecular Dynamics Simulation, 31P Spin-Lattice Relaxation, and Rigid-Body Dynamics. *Biophys. J.* **2008**, *94*, 3074−3083.
(47) Bertini, I.; Luchinat, C.; Parigi, G. Paramagnetic Constraints: An Aid for Quick Solution Structure Determination of Paramagnetic Metalloproteins. *Concepts Magn. Reson.* **2002**, *14*, 259−286.
(48) Schmitz, C.; John, M.; Park, A. Y.; Dixon, N. E.; Otting, G.; Pintacuda, G.; Huber, T. Efficient Chi-Tensor Determination and NH Assignment of Paramagnetic Proteins. *J. Biomol. NMR* **2006**, *35*, 79−87.
(49) Schmitz, C.; Stanton-Cook, M. J.; Su, X. C.; Otting, G.; Huber, T. Numbat: An Interactive Software Tool for Fitting Delta Chi-Tensors to Molecular Coordinates Using Pseudocontact Shifts. *J. Biomol. NMR* **2008**, *41*, 179−189.
(50) Pintacuda, G.; Park, A. Y.; Keniry, M. A.; Dixon, N. E.; Otting, G. Lanthanide Labeling Offers Fast NMR Approach to 3D Structure Determinations of Protein-Protein Complexes. *J. Am. Chem. Soc.* **2006**, *128*, 3696−3702.
(51) Pintacuda, G.; John, M.; Su, X. C.; Otting, G. NMR Structure Determination of Protein-Ligand Complexes by Lanthanide Labeling. *Acc. Chem. Res.* **2007**, *40*, 206−212.
(52) John, M.; Pintacuda, G.; Park, A. Y.; Dixon, N. E.; Otting, G. Structure Determination of Protein-Ligand Complexes by Transferred Paramagnetic Shifts. *J. Am. Chem. Soc.* **2006**, *128*, 12910−12916.
(53) Clore, G. M.; Tang, C.; Iwahara, J. Elucidating Transient Macromolecular Interactions Using Paramagnetic Relaxation Enhancement. *Curr. Opin. Struct. Biol.* **2007**, *17*, 603−616.
(54) Blumberg, W. Nuclear Spin-Lattice Relaxation Caused by Paramagnetic Impurities. *Phys. Rev.* **1960**, *119*, 79−84.
(55) Goldman, M. Impurity-Controlled Nuclear Relaxation. *Phys. Rev.* **1965**, *138*, A1675−A1681.
(56) Bloembergen, N. On the Interaction of Nuclear Spins in a Crystalline Lattice. *Physica* **1949**, *XV*, 386−426.
(57) Van Vleck, J. The Dipolar Broadening of Magnetic Resonance Lines in Crystals. *Phys. Rev.* **1948**, *74*, 1168−1183.
(58) Gaede, H. C.; Gawrisch, K. Lateral Diffusion Rates of Lipid, Water, and a Hydrophobic Drug in a Multilamellar Liposome. *Biophys. J.* **2003**, *85*, 1734−1740.
(59) Martinez-Seara, H.; Rog, T.; Pasenkiewicz-Gierula, M.; Vattulainen, I.; Karttunen, M.; Reigada, R. Effect of Double Bond Position on Lipid Bilayer Properties: Insight Through Atomistic Simulations. *J. Phys. Chem. B* **2007**, *111*, 11162−11168.
(60) Khutsishvili, G. R. *Proc. Inst. Phys. Acad. Sci. Georgia (USSR)* **1956**, *4*, 3.
(61) Lee, A. G. Lipid-protein Interactions. *Biochem. Soc. Trans.* **2011**, *39*, 761−766.
(62) Kessel, A.; Haliloglu, T.; Ben-Tal, N. Interactions of the M2delta Segment of the Acetylcholine Receptor with Lipid Bilayers: A Continuum-Solvent Model Study. *Biophys. J.* **2003**, *85*, 3687−3695.
(63) Kessel, A.; Shental-Bechor, D.; Haliloglu, T.; Ben-Tal, N. Interactions of Hydrophobic Peptides with Lipid Bilayers: Monte Carlo Simulations with M2delta. *Biophys. J.* **2003**, *85*, 3431−3444.
(64) Hung, A.; Tai, K.; Sansom, M. S. Molecular Dynamics Simulation of the M2 Helices Within the Nicotinic Acetylcholine Receptor Transmembrane Domain: Structure and Collective Motions. *Biophys. J.* **2005**, *88*, 3321−3333.
(65) Newstadt, J. P.; Mayo, D. J.; Inbaraj, J. J.; Subbaraman, N.; Lorigan, G. A. Determining the Helical Tilt of Membrane Peptides Using Electron Paramagnetic Resonance Spectroscopy. *J. Magn. Reson.* **2009**, *198*, 1−7.
(66) Marsh, D. Studies of Membrane Dynamics Using Nitroxide Spin Labels. *Pure Appl. Chem.* **1990**, *62*, 265−270.